Article

JOURNAL OF THERMOPLASTIC COMPOSITE MATERIAL

Journal of Thermoplastic Composite Materials
26(1) 109–124

DOI: 10.1177/0892705711419697
jtc.sagepub.com
SAGE

A simple procedure for the preparation of laponite and thermoplastic starch nanocomposites: Structural, mechanical, and thermal characterizations

Fauze A Aouada[1,2], Luiz HC Mattoso[2] and Elson Longo[1]

Abstract

The aim of this article is to propose advances for the preparation of hybrid nanocomposites prepared by the combination of intercalation from solution and melt-processing methods. This research investigates the effect of the laponite RDS content on the thermal, structural, and mechanical properties of thermoplastic starch (TPS). X-ray diffraction was performed to investigate the dispersion of the laponite RDS layers into the TPS matrix. The results show good nanodispersion, intercalation, and exfoliation of the clay platelets, indicating that these composites are true nanocomposites. The presence of laponite RDS also improves the thermal stability and mechanical properties of the TPS matrix due to its reinforcement effect which was optimized by the high degree of exfoliation of the clay. Thus, these results indicate that the exfoliated TPS–laponite nanocomposites have great potential for industrial applications and, more specifically, in the packaging field.

Keywords

Clay, mechanical properties, nanocomposites, reinforcement, thermal properties, X-ray

[1]Laboratório Interdisciplinar de Eletroquímica e Cerâmica (LIEC), Chemistry Institute, São Paulo State University, Araraquara, SP, Brazil
[2]National Nanotechnology Laboratory for Agriculture – LNNA – Embrapa Instrumentation – CNPDIA, São Carlos, SP, Brazil

Corresponding author:
Fauze A Aouada, Laboratório Interdisciplinar de Eletroqúumica e Cerâmica (LIEC), Chemistry Institute, São Paulo State University, Araraquara campus, 14801-907, Araraquara, SP, Brazil.
Email: faouada@yahoo.com.br

Introduction

The new group of composites, named as nanocomposites, is receiving a great deal of attention from different researchers in different fields.[1–4] In the nanocomposite materials at least one dimension of the particles is in the nanometer size (1–100 nm).[5] Additionally, when the domain size is equivalent to the dimension of a molecule, the atomic and molecular interactions can have a significant influence on the macroscopic properties of that material.[6]

The investigation of polymer/clay nanocomposites received considerable scientific and technological attention during the last years due to important clay properties, such as the high availability; the reinforcement effect even added into polymeric matrix in small quantities (1–5 wt%); and the huge knowledge regarding clay–polymer matrix intercalation chemistry.[7,8] For instance, Delhom et al.[9] developed a novel flame-retardant nanocomposite based on cellulose and clay materials. The authors observed that the nanocomposites show significant improvements in thermal properties, when compared with cellulose control sources; and tensile testing revealed an increase of approximately 80% in the ultimate stress of the cellulose/clay nanocomposites.

Laponite is a synthetic mineral with structure and composition similar to natural hectorite, which belongs to smectic group. The basic layered structures are composed by two external tetrahedral silica sheets and a central octahedral magnesia sheet.[10] Laponite RDS is a synthetic hectorite with aspect ratio of 20–30[6] and chemical formula – $Si_8Mg_{85.45}Li_{0.4}H_4O_{24}Na_{0.7}$ + $Na_4P_2O_7$. Since $Na_4P_2O_7$ peptizer is mixed to the laponite aiming to increase their stability in aqueous solution.[11]

Starch is a no thermoplastic polysaccharide, but in the presence of plasticizers such as glycerol[12] at high temperatures and under shear, it can readily melt and flow, facilitating its use as extruded or injected material, which is similar to most conventional synthetic thermoplastic polymers.[13] Thermoplastic starch (TPS) is thus derived from renewable sources. It is a rather inexpensive material compared to synthetic thermoplastics and can easily be processed with plastic-processing machines. However, TPS shows a number of shortcomings that could limit or restrict their industrial application (e.g., packaging)[14] such as moisture sensitivity and lower mechanical properties. To overcome these shortcomings, inorganic–organic nanocomposites have been prepared by the addition of clay into the TPS matrix.

The aim of this article is to propose advances in the preparation of hybrid nanocomposites prepared through the combination of intercalation from solution and melt-processing preparation methods to be applied in the packaging field. The effect of the laponite RDS on the thermal, structural, and mechanical properties of the nanocomposites was investigated. The combination of the both methods has not been applied to prepare the TPS–laponite RDS nanocomposites.

Experimental

Materials

Regular corn starch containing 28% amylose (Amidex 3001 TM) and laponite RDS were acquired by Corn Products Brasil Ltd and Southern Clay Products, Inc., respectively. Glycerol was purchased from Aldrich. All chemicals were used as received.

Preparation of TPS and laponite RDS nanocomposites

The TPS and laponite RDS nanocomposites were obtained from combination of intercalation from solution and melt-processing preparation methods. The content of starch and glycerol was fixed at 70 and 30 wt%, respectively. The content of laponite RDS was 1, 2, 3, and 5 wt% based on the total starch and glycerol weight. Corn starch powder was first dried overnight at 70°C in a ventilated oven to remove the free water.

In the first step, a known quantity of laponite RDS was introduced into 200 mL of distilled water and dispersed in an ultrasonic bath at 25°C for 2 h. Then, the corn starch was dispersed into laponite RDS dispersion under magnetic stirring for 10 min. The glycerol was slowly added into the same solution under stirring. After the complete addition of glycerol, the mixture was mixed at high speed (1500 rpm) to obtain a homogeneous dispersion. The mixture was placed in a ventilated oven at 90°C for 24 h, which facilitated vaporization of the bound water and diffusion of the glycerol into the starch granules.

In the second step, the mixtures were processed in a Haake Rheomix 600 batch mixer connected to a torque rheometer with roller-like rotors. In this process, some external parameters could influence the plasticization of the starch such as temperature, rotor speed, and residence time. These parameters were initially studied to reveal optimal conditions: temperature = 120–160°C; rotor speed = 50–200 rpm; and residence time = 6–20 min. After processing, mechanical properties (tensile stress, elastic modulus, and elongation at the break) and physical aspects after final molding (flexibility, rigidity, and homogeneity) of the TPS (without laponite) were investigated (data are not shown). The optimal condition was then determined (120°C, 50 rpm, and 20 min) and fixed for nanocomposite processing.

Characterization of nanocomposites

Field Emission Scanning Electron Microscopy. The TPS and TPS nanocomposites surfaces were characterized by high-resolution Field Emission Scanning Electron Microscopy (FE-SEM; Zeiss SUPRA 35). The samples were fractured under liquid nitrogen, dried at 60°C for 1 day under vacuum, and adhered onto an aluminum stub covered with a thin silver layer.

X-Ray diffraction. The X-Ray diffraction (XRD) studies of the laponite RDS, TPS, and nanocomposites were carried out using a Rigaku D/Max 2500PC X-ray diffractometer (40 kV, 150 mA) equipped with Cu K_α radiation (λ = 0.15406 nm) and a curved graphite crystal monochromator. All experiments were carried out at ambient temperature with a scanning rate of 0.5/min and a step size of 0.02° in the range of 2θ = 3–30°.

Thermogravimetric analysis. The thermogravimetric analysis (TGA) was carried out using TGA Q-500 equipment from TA Instruments (New Castle, United States) from room temperature to 700°C (or 973.15 K) at a heating rate of 10°C/min under nitrogen flow of 60 mL/min. An initial thermal degradation temperature (T_d initial) was reported by the onset degradation temperature where the weight loss started to occur.[15] The maximum thermal degradation temperature ($T_{d\ maximum}$) was calculated using maximum values of derivative thermogravimetric (DTG) curves of the specimens.

Mechanical properties of nanocomposites. Mechanical properties (tensile strength, Young's modulus, and elongation at the break) were determined on nanocomposites previously conditioned for 14 days at 53% RH (relative humidity percentage) and room temperature using an Universal Testing Machine (Model EMIC DL 500 MF) according to ASTM standard D638 for tensile properties: specimen type IV and articulated screw action grips for maximum capacity of 500N (50 kgf) – code EMIC GR018. Tensile strength was calculated by dividing the maximum load for breaking film by the original cross-sectional area of the sample. Elongation at break was calculated by dividing the difference in the length at the moment of rupture by the original length of the sample or initial gage length and multiplying by 100. Young's modulus values were calculated by the slope of the initial linear range of the stress–strain curve. The measurements were conducted using an extensometer with a 50 kgf load cell operating at 10 mm/min crosshead speed. Measurements were performed in replicate to check reproducibility; error bars indicate the standard deviation (n = 5).

Results and discussion

TPS–laponite RDS nanocomposites formation

The thermoplastic process is well related in the literature.[15] Basically, the process is composed by transformation of the semicrystalline starch granule into homogenous material applying shear and heat in the presence of plasticizer agent. The process occurs through of destruction of hydrogen bonds between the starch molecules with new formation of hydrogen bonds between the plasticizer and starch.

In this study, we reported the preparation of TPS and TPS–laponite RDS nanocomposites through the combination of the following

Scheme 1. Illustration of possible states of dispersion of laponite RDS into thermoplastic starch (TPS) matrix.

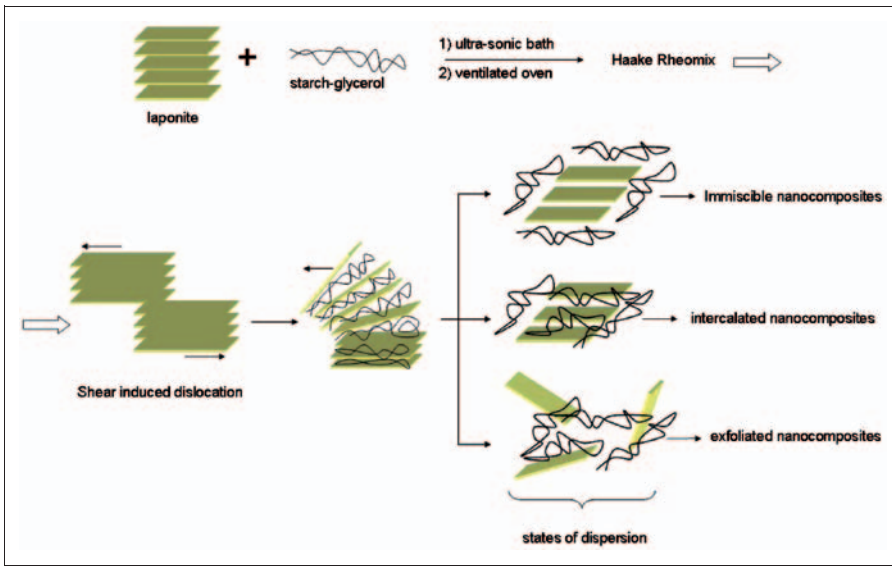

methods: (a) intercalation from the solution and (b) melt-processing. The illustration of possible states of dispersion of laponite RDS into TPS matrix is shown in Scheme 1.

Evolution of nanocomposites formation by melt viscosity using torque curves

Torque, temperature, and energy as a function of time for TPS and TPS nanocomposites were monitored during the processing. Figure 1(a) shows a decrease in the torque values for TPS until they reach a plateau around 2 min and remains constant until the conclusion of the experiment. The TPS did not present a thermoplasticization stage, indicating that this stage was reached in the first step of nanocomposite preparation; that is, intercalation from solution.

In contrast, TPS nanocomposites presented different behaviors. The torque increased after 2 min and continued to increase for 12–16 min, depending on the laponite RDS content in the TPS matrix. This result indicates a steady increase in viscosity for this sample,[16] indicating that the second step of the processing (melt-processing preparation) is necessary to complete the destruction, plasticization, and homogenization of starch structures.

The melt temperature, shown in Figure 1(b), increased over time and reached final temperature around 115–123°C. This range value is very close to the initial temperature of the mixing chamber fixed at 120°C. In addition, in this temperature range, significant degradations of TPS and laponite RDS molecules were not expected (see the TGA section). The variation in energy as a function of residence

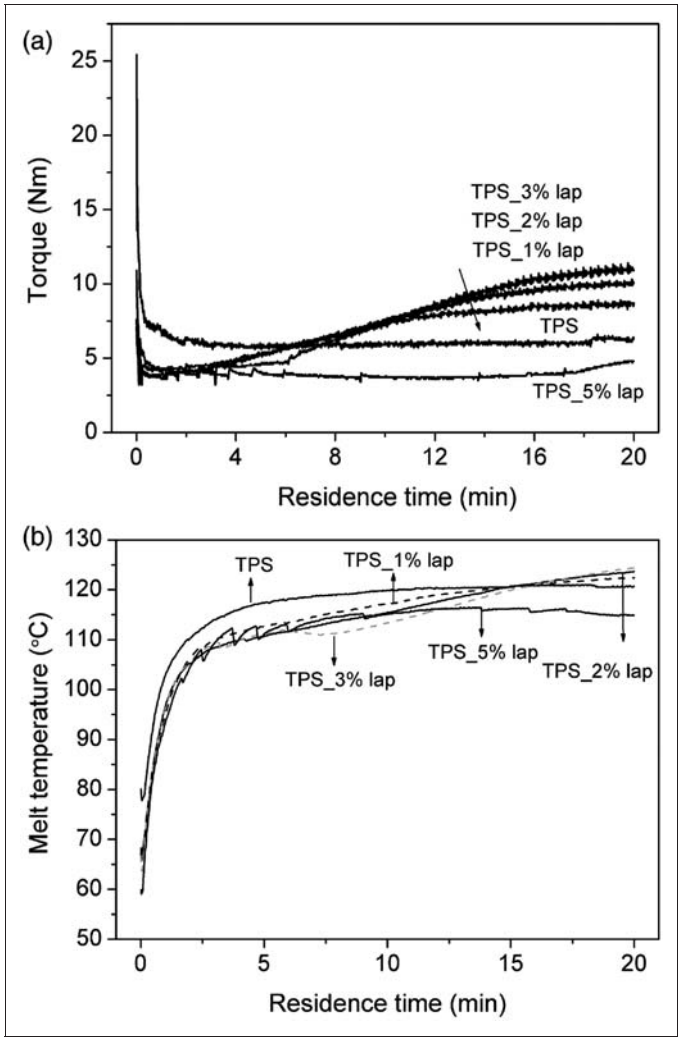

Figure 1. Torque (a), temperature of melting (b), and energy (c) curves for thermoplastic starch (TPS) and TPS–laponite RDS nanocomposites obtained by processing in a Haake Rheomix at 120°C at a speed of 50 rpm for 20 min.

time (processing time) for the same nanocomposites is shown in Figure 1(c). The TPS energy increases linearly with processing time; the required energy for TPS processing after 20 min was 38.4 kJ. This behavior could be related to the torque changes (viscosity) as previously discussed (see Figure 1(a)). The required energies for TPS processing were dependent on the laponite RDS content. The energy values were 42.8, 45.8, and 46.1 kJ for laponite RDS concentrations of 1, 2, and 3 wt%.

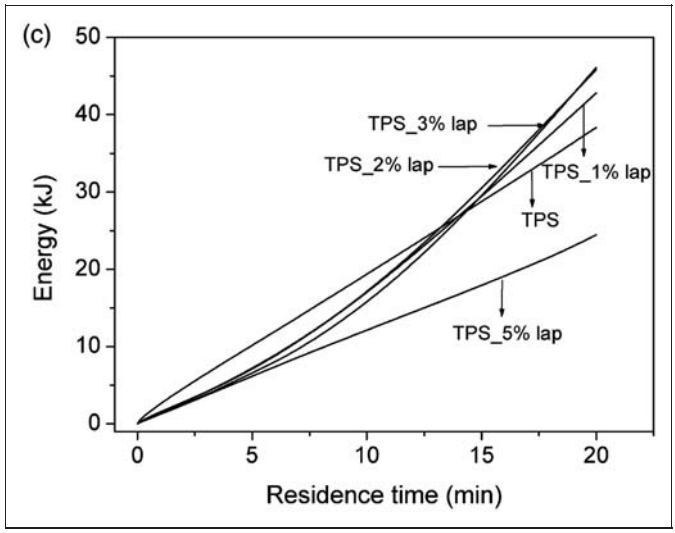

Figure 1. Continued.

Unexpectedly, the TPS with 5% laponite RDS presented the lowest energy, torque, and melt-temperature values. Possibly the high amount of laponite RDS in the TPS matrix contributes to the dispersion of energy inside laponite galleries, which could facilitate processing whereby both torque and melt-temperature values decrease. Another effect that may be corelated is the decrease in the viscosity of the melting.

Dispersion investigation by XRD

To investigate the dispersion of the laponite RDS layers in the TPS polymer matrix, XRD analyses were performed on the nanocomposites. The diffraction pattern for laponite RDS clay powder is shown in Figure 2. The pattern is consistent with a montmorillonoid-type powder pattern showing some disorder in the clay. In addition, several sharp diffraction peaks due to $Na_4P_2O_7$ are also observed[17] at $2\theta = 19.64^\circ$ (basal d-spacing (d) = 0.45 nm); $2\theta = 20.11^\circ$ (d = 0.44 nm); and $2\theta = 26.46^\circ$ (d = 0.34 nm). The basal spacing of laponite RDS was calculated from Bragg's equation, $\lambda = 2d \sin \theta$. An intensive peak at $2\theta = 6.40^\circ$ corresponds to an interlayer basal spacing of 1.38 nm. In all XRD patterns of the nanocomposites, no diffraction peaks between $2\theta = 3$–12° (Figure 2(b)) were observed, indicating a good nanodispersion and exfoliation of the clay platelets, that is, separated platelets dispersed individually in the TPS matrix. According to Delhom et al.,[9] the lack of a diffraction peak for the one specific composite with clay is a good indication that this composite is a true nanocomposite with the polymer intercalated with the exfoliated clay nanospecimens.

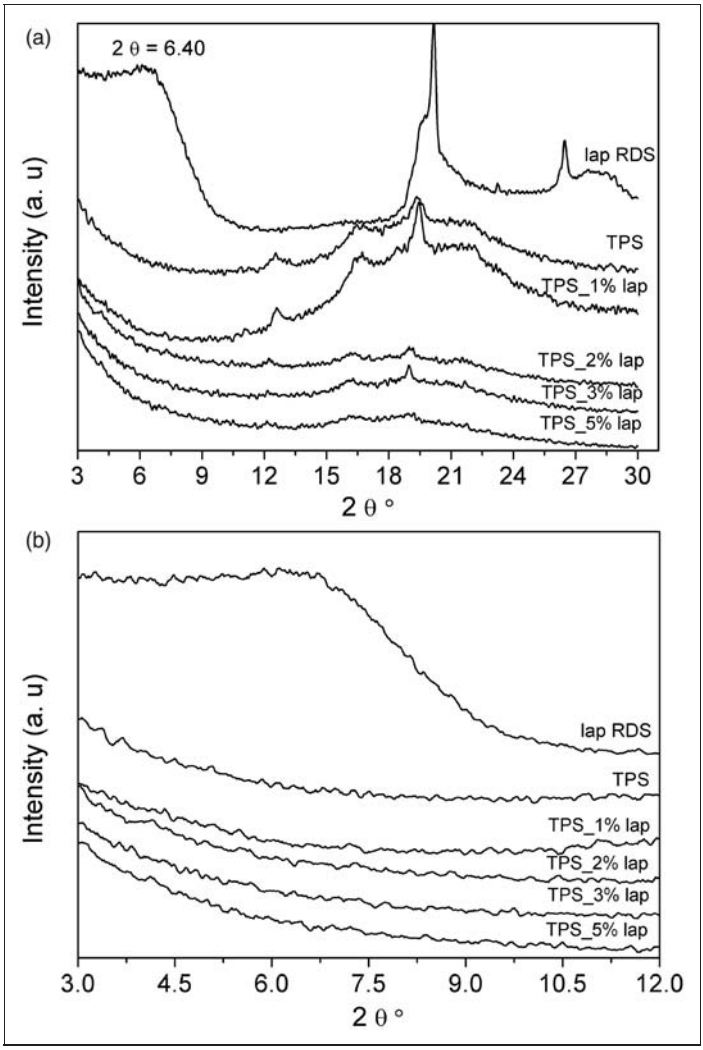

Figure 2. (a) X-Ray diffraction (XRD) patterns of the laponite RDS, thermoplastic starch (TPS), and TPS–laponite RDS nanocomposites and (b) XRD patterns expanded in the $2\theta = 3–12^{\circ}$ region showing the nanodispersion/exfoliation of the clay platelets.

Morphologic investigation by FE-SEM

Figure 3(a) and (b) show FE-SEM micrographs of TPS and TPS–laponite RDS nanocomposites containing 2% laponite. A homogeneous surface is observed for both figures, indicating that the starch granules were completely disrupted and the laponite was well dispersed in the polymer matrix. All TPS–laponite

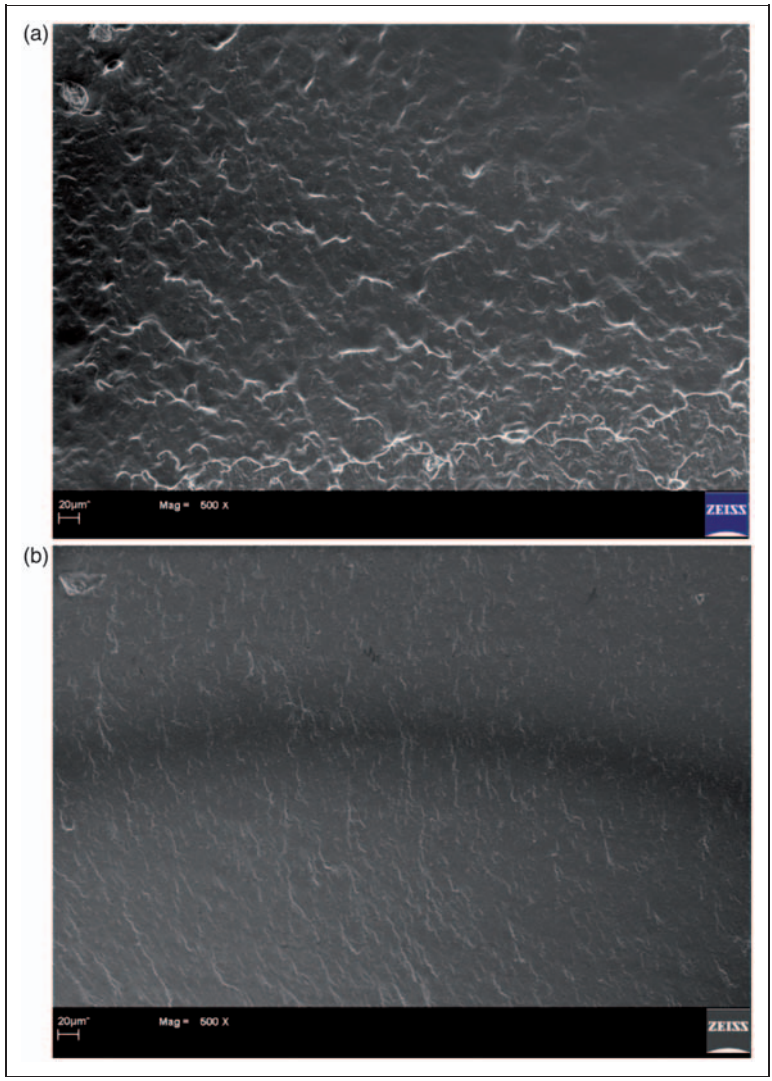

Figure 3. Scanning electron microscope (SEM) micrographs of the fractured surface: (a) thermoplastic starch (TPS) and (b-c) TPS–laponite RDS nanocomposites containing 2 wt% laponite at two different magnifications.

nanocomposites presented similar morphologies so their micrographs are not shown. Similar behavior was observed in the laponite RD dispersed into biodegradable starch described by Chung et al.[18] In addition, there was no phase separation between laponite–TPS specimens, and no clay aggregation can be seen even at higher magnifications (see Figure 3(c)), which is a strong indication of good interaction, compatibility, and miscibility between them and confirms well-dispersed nanocomposites.

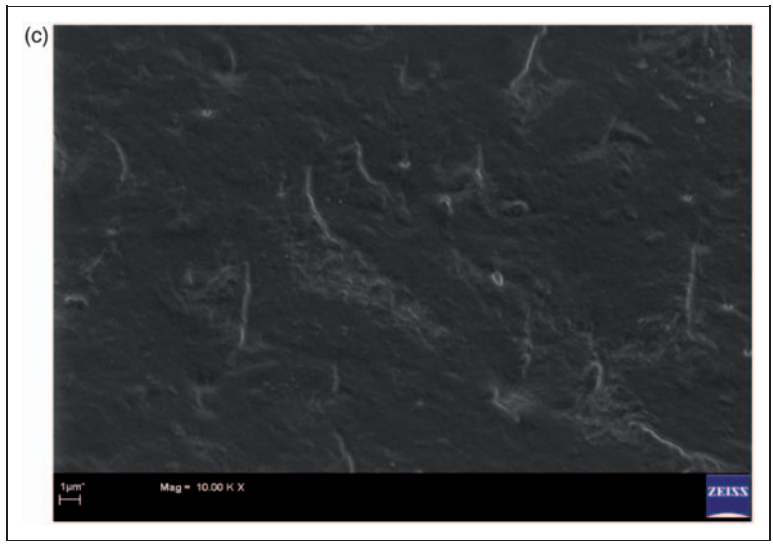

Figure 3. Continued.

Thermal degradation investigation by TGA

Thermal degradation during the processing of starch and starch nanocomposites is an important issue. The TGA has been the conventional and most popular technique used to study the thermal stability and decomposition of starches and their nanocomposites.[19–21] Figure 4 shows TGA and DTG results of TPS and TPS nanocomposites with 1–5% laponite RDS. Table 1 showed that the onset temperature ($T_{d\ initial}$) of TPS degradation increased from 175°C (or 448.15 K) to around 200°C (or 473.15 K), indicating an increase in the thermal stability when the laponite was incorporated in the TPS matrix. This improvement has been documented by other researchers. For instance, Zaidi et al.[21] observed similar behaviors in the thermal analysis of cloisite-PLA nanocomposites. The authors attributed the improvement of the thermal stability due to the strong interaction between the clay and the polymer matrix. Table 1 also shows that the nanocomposite maximum degradation temperature ($T_{d\ maximum}$) decreased slightly as compared to the TPS. In accordance to the Baniasadi et al.,[20] possible reasons can be related to this effect. Firstly, the stacked silicate layers could sustain accumulated heat and accelerate the degradation process; and secondly, the clay itself can also catalyze the degradation of polymer matrices.

The decomposition activation energies (E_t) of the TPS and nanocomposites were calculated from TGA curves by the integral method adapted from Horowitz et al.[22]

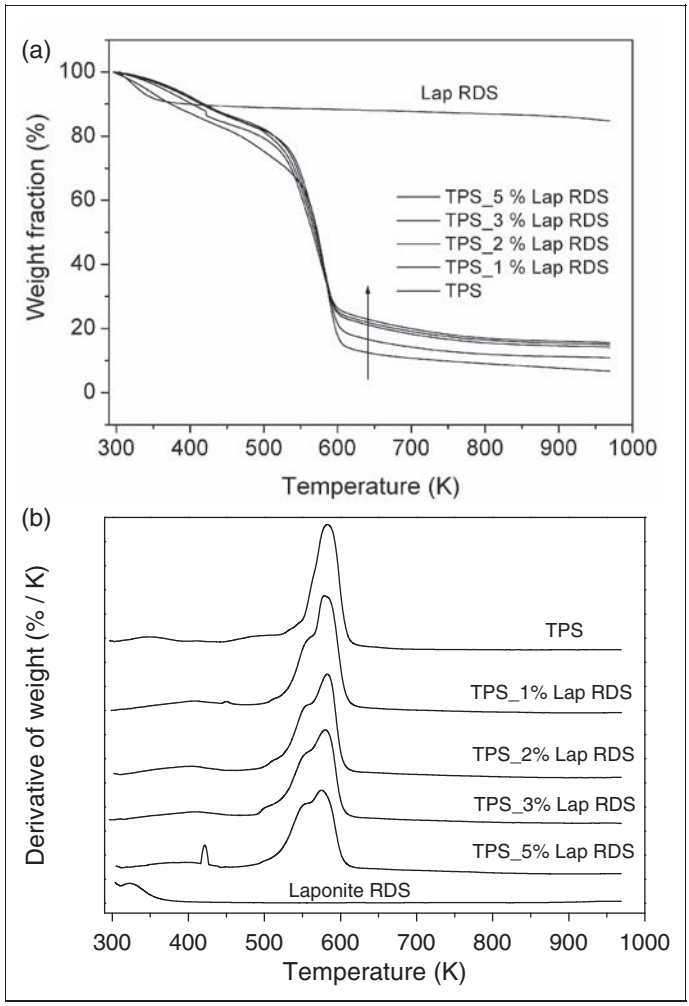

Figure 4. (a) Thermogravimetric analysis (TGA) and (b) derivative thermogravimetric (DTG) curves of thermoplastic starch (TPS) and TPS–laponite RDS nanocomposites prepared at different laponite RDS contents (1–5 wt%).

as shown in Equation (1):

$$\ln[\ln(1-\alpha)^{-1}] = \frac{E_t \theta}{RT^2_{ini}} \quad (1)$$

where α is the decomposed fraction, T_{ini} is the initial decomposition temperature, θ is the difference between $T - T_{ini}$, and R is the gas constant.

Figure 5 shows the plots of ln [ln $(1 - \alpha)^{-1}$] versus θ, and E_t can be calculated using the slope. The E_t values were 10.60; 11.50; 11.03; 11.42; and 9.49 kJ/mol for

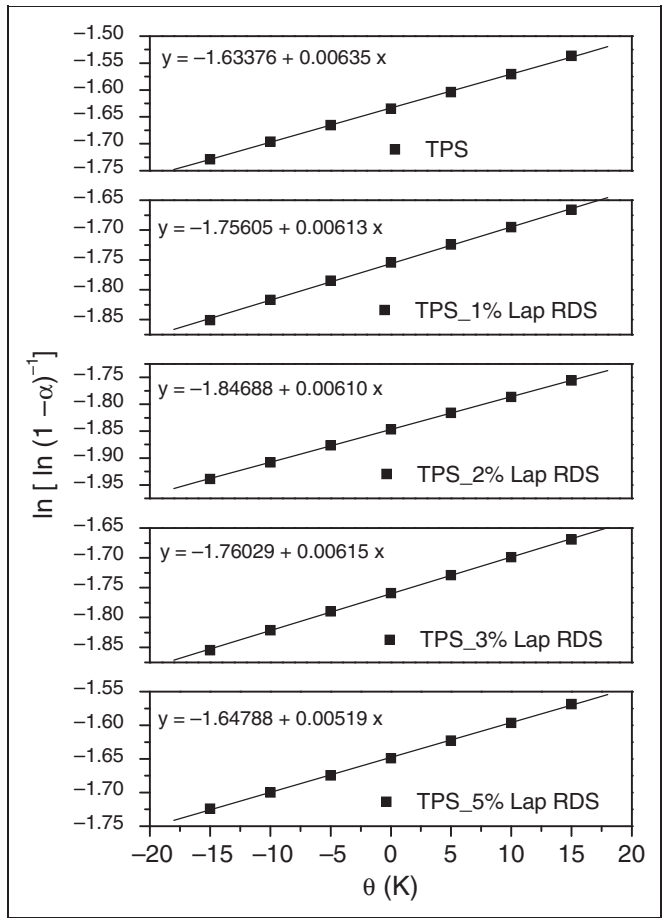

Figure 5. Plots of ln [ln $(1 - \alpha)^{-1}$)] versus θ for the determination of E_t.

nanocomposites prepared with 0; 1; 2; 3; and 5 wt% laponite RDS. The increase in the laponite RDS content caused an increased in E_t values, which confirms the improvement in the thermal stability of the TPS matrix up to 3% laponite. Despite of their high initial decomposition temperature (Table 1), the TPS 5% lap had E_t values lower than TPS. Probably, the decrease in E_t is related to the low dependence between ln [ln$(1 - \alpha)^{-1}$] and θ, indicated by the low slope showed in Figure 5.

Mechanical properties

Tensile strength, Young's modulus and elongation at the break properties were determined to evaluate the influence of laponite RDS on the mechanical behavior of TPS nanocomposites. Figure 6 shows the stress–strain curves for TPS and TPS–laponite RDS nanocomposites prepared at different laponite

Table 1. Thermal stability parameters of TPS and TPS–laponite RDS nanocomposites obtained from TGA technique.

Nanocomposite	$T_{dinitial}$* (K)	$T_{dmaximum}$ (K)	T_{dfinal} (K)
TPS	448.05	583.15	626.25
TPS_1% lap	474.95	578.55	628.65
TPS_2% lap	466.25	582.85	629.75
TPS_3% lap	472.65	580.05	630.55
TPS_5% lap	468.85	574.95	630.25

TPS: thermoplastic starch, TGA: thermogravimetric analysis.
*$T_{dinitial}$ or T_{ini}.

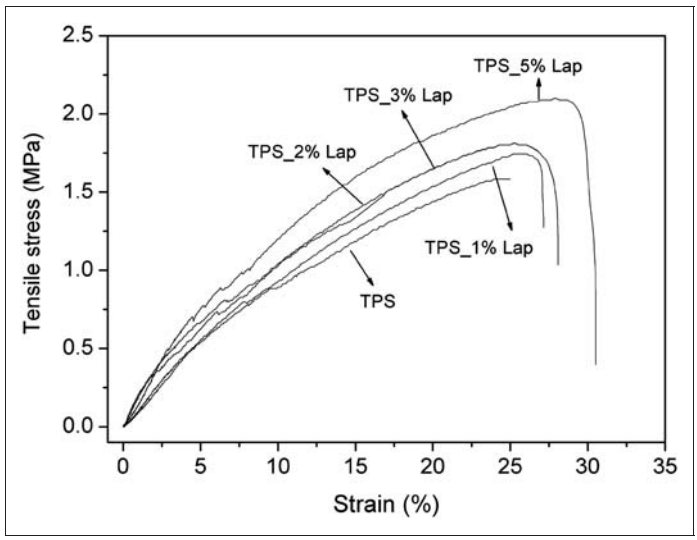

Figure 6. The stress–strain curves for thermoplastic starch (TPS) and TPS–laponite RDS nanocomposites prepared at different laponite contents (1–5 wt%).

contents (1–5 wt%). Table 2 showed that mechanical properties were improved by the addition of laponite RDS. Tensile strength slightly varied from 1.7 ± 0.2 to 2.0 ± 0.1 MPa; but the Young's modulus varied significantly from 11.3 ± 0.9 to 16.3 ± 0.6 MPa. The improvement in these properties may be due to good dispersion of the clay platelets into the TPS matrix, which increases the reinforcement degree due to the high interaction between the clay and the TPS matrix. This tendency was also observed by Zhao et al.,[23] where the authors showed that mechanical properties of the polyamide 12/montmorillonite nanocomposites are very sensitive to the degree of clay dispersion in the polymer matrix.

Although mechanical properties improve with the addition of laponite into the TPS matrix, the effect on elongation at the break was not significant (average

Table 2. Mechanical properties of TPS and TPS–laponite RDS nanocomposites obtained from tensile tests.

Nanocomposite	Tensile strength (MPa)	Young's modulus (MPa)	Elongation at break (%)
TPS	1.7 ± 0.2	11.3 ± 0.9	25.0 ± 3.6
TPS_1% lap	1.7 ± 0.1	12.8 ± 2.9	25.4 ± 2.4
TPS_2% lap	1.8 ± 0.2	16.1 ± 1.4	27.9 ± 4.2
TPS_3% lap	1.8 ± 0.1	15.7 ± 1.7	27.9 ± 4.2
TPS_5% lap	2.0 ± 0.1	16.3 ± 0.6	30.3 ± 4.0

TPS: thermoplastic starch.

values around 30%). This is an indicative that the TPS and TPS nanocomposites had practically the same flexibility; a very important key in the industrial field (mainly in packaging applications). In addition, several authors related the diminishing of the elongation at the break of the polymeric nanocomposites with the addition of inorganic clay,[23,24] which may restrict their industrial application.

Conclusions

It was possible to obtain TPS and TPS–laponite RDS nanocomposites through a simple procedure involving the combination of intercalation from solution and melt-processing preparation methods. In XRD spectra of the nanocomposites, no diffraction peaks between $2\theta = 3$–12° (corresponding to the laponite RDS diffraction peak) were observed, indicating a good nanodispersion and intercalation of the clay platelets. In addition, this result is a good indication that the TPS–laponite RDS composite is a true nanocomposite with the polymer intercalated with the exfoliated clay nanospecimens.

The presence of laponite RDS improved the thermal stability and mechanical properties of the TPS matrix due to the reinforcement effect of the laponite maximized by a high interaction with the TPS matrix. As a consequence, the Young's modulus varied from 11.3 ± 0.9 to 16.3 ± 0.6 MPa, when the laponite RDS amount was increased from 0 to 5 wt%. These results indicate that TPS–laponite RDS nanocomposites with a good degree of exfoliation have great potential for industrial applications (more specifically in the packaging field).

Funding

The authors are grateful to Instituto Nacional de Ciências dos Materiais em Nanotecnologia (INCTMN), National Council for Scientific and Technological Development (CNPq-Brazil), Foundation for Research Support of São Paulo (FAPESP), FINEP/MCT for their financial support and fellowships.

References

1. Phua YJ, Chow WS and Mohd Ishak ZA. Poly(butylene succinate)/organo-montmorillonite nanocomposites: Effects of the organoclay content on mechanical, thermal, and moisture absorption properties. *Journal of Thermoplastic Composite Materials* 2011; 24(1): 133–151.
2. Ibrahim SM. Characterization, mechanical, and thermal properties of gamma irradiated starch films reinforced with mineral clay. *Journal of Applied Polymer Science* 2011; 119(2): 685–692.
3. Reyna-Valencia A, Deyrail Y and Bousmina M. In situ follow-up of the intercalation process in a clay/polymer nanocomposite model system by rheo-XRD analyses. *Macromolecules* 2010; 43(1): 354–361.
4. Dwivedi M, Alam S and Ghosh AK. Correlation in morphology and thermal behavior of nanoclay-reinforced polyetherimide nanocomposites. *Journal of Thermoplastic Composite Materials* 2011; 24(2): 265–280.
5. Pavlidou S and Papaspyrides CD. A review on polymer-layered silicate nanocomposites. *Progress in Polymer Science* 2008; 33(12): 1119–1198.
6. Rao Y. Gelatin–clay nanocomposites of improved properties. *Polymer* 2007; 48(18): 5369–5375.
7. Krishnamoorti R and Vaia RA. Polymer nanocomposites. *Journal of Polymer Science Part B-Polymer Physics* 2007; 45(24): 3252–3256.
8. Rousseaux DDJ, Sclavons M, Godard P and Marchand-Brynaert J. Carboxylate clays: A model study for polypropylene/clay nanocomposites. *Polymer Degradation and Stability* 2010; 95(7): 1194–1204.
9. Delhom CD, White-Ghoorahoo LA and Pang SS. Development and characterization of cellulose/clay nanocomposites. *Composites Part B-Engineering* 2010; 41(6): 475–481.
10. Liu J, Lee J-B, Kim D-W and Kim Y. Preparation of high concentration of silver colloidal nanoparticles in layered laponite sol. *Colloids and Surfaces A: Physicochemical and Engineering Aspects* 2007; 302(1–3): 276–279.
11. Boucenna I, Royon L and Colinart P. Effect of laponite clay particles on thermal and rheological properties of pluronic triblock copolymer. *Journal of Thermal Analysis and Calorimetry* 2009; 98(1): 119–123.
12. Sankri A, Arhaliass A, Dez I, Gaumont AC, Grohens Y, Lourdin D, Pillin I, Rolland-Sabaté A and Leroy E. Thermoplastic starch plasticized by an ionic liquid. *Carbohydrate Polymers* 2010; 82(2): 256–263.
13. Forssell PM, Mikkilä JM, Moates GK and Parker R. Phase and glass transition behaviour of concentrated barley starch-glycerol-water mixtures, a model for thermoplastic starch. *Carbohydrate Polymers* 1997; 34(4): 275–282.
14. Bocchini S, Battegazzore D and Frache A. Poly (butylensuccinate co-adipate)-thermoplastic starch nanocomposite blends. *Carbohydrate Polymers* 2010; 82(3): 802–808.
15. Prachayawarakorn J, Sangnitidej P and Boonpasith P. Properties of thermoplastic rice starch composites reinforced by cotton or low-density polyethylene. *Carbohydrate Polymers* 2010; 81(2): 425–433.
16. Lima FF and Andrade CT. Effect of melt-processing and ultrasonic treatment on physical properties of high-amylose maize starch. *Ultrasonics Sonochemistry* 2010; 17(4): 637–641.
17. Majumdar D, Blanton TN and Schwark DW. Clay-polymer nanocomposite coatings for imaging application. *Applied Clay Science* 2003; 23(5–6): 265–273.

18. Chung Y-L, Ansari S, Estevez L, Hayrapetyan S, Giannelis EP and Lai H-S. Preparation and properties of biodegradable starch-clay nanocomposites. *Carbohydrate Polymers* 2010; 79(2): 391–396.
19. Liu H, Xie F, Yu L, Chen L and Li L. Thermal processing of starch-based polymers. *Progress in Polymer Science* 2009; 34(12): 1348–1368.
20. Baniasadi H, Ramazani A and Nikkhah SJ. Investigation of in situ prepared polypropylene/clay nanocomposites properties and comparing to melt blending method. *Materials & Design* 2010; 31(1): 76–84.
21. Zaidi L, Kaci M, Bruzaud S, Bourmaud A and Grohens Y. Effect of natural weather on the structure and properties of polylactide/cloisite 30B nanocomposites. *Polymer Degradation and Stability* 2010; 95(9): 1751–1758.
22. Horowitz HH and Metzger GA. A new analysis of thermogravimetric traces. *Analytical Chemistry* 1963; 35(10): 1464.
23. Zhao F, Bao X, McLauchlin AR, Gu J, Wan C and Kandasubramanian B. Effect of POSS on morphology and mechanical properties of polyamide 12/montmorillonite nanocomposites. *Applied Clay Science* 2010; 47(3–4): 249–256.
24. Uddin MF and Sun CT. Improved dispersion and mechanical properties of hybrid nanocomposites. *Composites Science and Technology* 2010; 70(2): 223–230.